Published in final edited form as:

FASEB J. 2020 September ; 34(9): 11714–11728. doi:10.1096/fj.201902254RR.

Aldosterone-induced microRNAs act as feedback regulators of mineralocorticoid receptor signaling in kidney epithelia.

N. Ozbaki-Yagan[1], **X. Liu**[1], **A.J. Bodnar**[2], **J. Ho**[2], **M.B. Butterworth**[1,*]

[1]Department of Cell Biology, University of Pittsburgh, Pittsburgh, PA, USA

[2]Division of Nephrology in the Department of Pediatrics, University of Pittsburgh, Pittsburgh, PA, USA

Abstract

The final steps in the Renin-Angiotensin-Aldosterone signaling System (RAAS) involve binding of the corticosteroid hormone, aldosterone to its mineralocorticoid receptor (MR). The bound MR interacts with response elements to induce or repress the transcription of aldosterone-regulated genes. A well characterized aldosterone-induced gene is the serum and glucocorticoid induced kinase (SGK1) which acts downstream to increase sodium transport in distal kidney nephron epithelial cells. The role of microRNAs (miRs) induced by extended aldosterone stimulation in regulating MR and SGK1 has not been reported. In these studies, miRs predicted to bind to the 3'-UTR of mouse MR were profiled by qRT-PCR after aldosterone stimulation. The miR-466a/b/c/e family was upregulated in mouse kidney cortical collecting duct epithelial cells. A luciferase reporter assay confirmed miR-466 binding to both MR and SGK1 3'-UTRs. Inhibition of miR-466 increased MR and SGK1 mRNA and protein levels. Inhibiting miR-466b and preventing its upregulation after aldosterone stimulation increased amiloride-sensitive sodium transport and sensitivity to aldosterone stimulation. *In vivo* up-regulation of miR-466 was confirmed in distal nephrons of mice on low Na^+ diets. Repression of MR and SGK1 by aldosterone-induced miRs may represent a negative feedback loop that contributes to a form of aldosterone escape *in vivo*.

Keywords

steroid hormone; mineralocorticoid receptor; kidney collecting duct; epithelial sodium channel

Introduction

Inappropriately elevated levels of the mineralocorticoid steroid hormone aldosterone lead to the development of hypertension(1-3). Aldosterone is the final constituent of the renin-angiotensin-aldosterone (RAAS) signaling cascade(4-7). Aldosterone is produced in the

*Corresponding Author Department of Cell Biology, University of Pittsburgh School of Medicine, S314 BST, 200 Lothrop St., Pittsburgh, PA, 15261, Phone: 412-383-8591, Fax: 412-648-8330, michael7@pitt.edu.

Author Contributions

NOY - performed the research, analyzed data, wrote the paper

XL - performed the research, analyzed data,

AJB - performed the research, analyzed data

JH – designed research, wrote the paper

MBB - designed research, performed the research, analyzed data ,wrote the paper

zona glomerulosa cells of the adrenal gland in response to renin, which is released when plasma sodium (Na^+) or blood volume is low(8-11). By binding to the mineralocorticoid receptor (MR) aldosterone induces the transcription of proteins that function together to establish a coordinated cellular genomic response(12, 13). The purpose of the final signaling step is to increase Na^+ reabsorption from glomerular filtrate. Homeostatic feedback following aldosterone stimulation reverses the signaling cascade as the cues to release aldosterone (reduced plasma volume or lower Na^+ levels) are diminished when plasma Na^+ and volume are restored(14-16). There are known cellular mechanisms that reverse aldosterone's action and keep the signaling cascade in check. Studies have demonstrated that aldosterone stimulation results in post-translational modifications to the MR that cause its degradation(17, 18). A recent study demonstrated that mRNA expression of MR was reduced in response to long term aldosterone stimulation(19). A decrease in MR would diminish the ability to elicit a full aldosterone stimulation and protect the cells from aldosterone excess. A major aldosterone-induced protein is the serum and glucocorticoid kinase (SGK1). SGK1 is responsible for transducing many of the cellular responses to aldosterone stimulation and coordinates the upregulation of Na^+ transport via a number of channels and transporters(20-23). The rapid induction of SGK1 mRNA is not accompanied by an equivalent change in protein expression(24). This moderated cellular response protects the cells from dramatic swings in SGK1 action. The actions of aldosterone are considered pleiotropic with different cellular responses noted in different cell and tissue types, given the same hormonal input(25-27). The post-transcriptional regulation by microRNAs could account for both the restriction of aldosterone signaling (feedback regulation), and the heterogeneous actions of the hormone noted in prior studies.

MicroRNAs (miRs) are non-coding RNAs between 18-23 nucleotides long and function primarily to degrade target mRNA and prevent protein synthesis(28-32). Precursor miRs are synthesized in the nucleus, either embedded in the introns (and occasionally the exons) of protein coding genes or encoded as stand-alone and cluster miRs driven by promotors and enhancers specifically regulating the production of the miRs(33-36). Aldosterone can induce or repress miRs, and mineralocorticoid response elements have been noted upstream of aldosterone-induced miRs that would account for their upregulation(37-39). Precursor miRs are exported to the cytoplasm for processing by the endonuclease Dicer(31, 40-44). Dicer processes the stem-loop RNA structure to produce a mature miR strand that is loaded into an inhibitory RNA-Induced Silencing Complex (RISC) with a second endonuclease, Argonaute(45-47). RISC is responsible for target recognition by sequence complementarity of the miRs with mRNAs, mainly in the mRNA 3'-untranslated regions (3'-UTRs)(48-50). The targeted mRNA is degraded by the RISC or protein translation is sterically hindered by binding of the RISC to the mRNA so that efficient protein synthesis is interrupted. The net result is a decrease in the steady-state protein level due to the binding of miRs. It is considered that the majority of protein coding mRNAs are targeted by miRs, and that non-coding RNAs (including miRs) regulate up to 80% of all protein coding genes(51-53). MiRs have been shown to target constituents of the RAAS cascade. Production of signaling hormones, expression of receptors and signaling proteins are all impacted by changes in miR expression(39, 54-59). However, the ability for aldosterone-induced miRs to feedback and alter the effectors of RAAS signaling has not been systematically investigated.

In this study we report on a family of miRs, mmu-miR-466, that are coordinately upregulated in principal epithelial cortical collecting duct (CCD) cells of the distal nephron in response to extended aldosterone stimulation. The miRs' targets, as demonstrated using a dual luciferase reporter assay, include MR and SGK1. Binding of miR-466 reduces the production of both proteins. By inhibiting miR-466 using antagomirs this repression is relieved and the protein levels of both MR and SGK1 are elevated after aldosterone stimulation. Sensitivity to extended aldosterone exposure, as measured by the amiloride-sensitive short circuit current activity in cultured mCCD-cl1 cells, is greater when the miR upregulation is prevented. A similar increase in miR-466 expression was observed *in vivo* in CCD cells isolated from mice placed on low Na^+ diets to stimulate aldosterone release. These miRs contribute to a negative feedback loop that dampens long-term aldosterone signaling. This would constitute a form of aldosterone escape that reduces cellular sensitivity to aldosterone to protect aldosterone-sensitive tissues from excessive aldosterone exposure.

Material and Methods

Antibodies and Reagents

All chemicals were purchased from Sigma-Aldrich (St. Louis, MO) or Thermo Fisher (Pittsburgh, PA) unless noted otherwise. Antibodies used are as follows: anti-mineralocorticoid receptor (mouse monoclonal, anti-rat, isotype MIgG1, kappa light chain from the Developmental Studies Hybridoma Bank (DSHB) at the University of Iowa. The hybridoma was deposited to the DSHB by Gomez-Sanchez, C. (DSHB Hybridoma Product rMR1-18 1D5). Anti-tubulin (mouse monoclonal, anti-*Tetrahymena thermophila* and *Tetrahymena pyriformis* (mixture), isotype MIgG1 from the DSHB at the University of Iowa. The hybridoma was deposited to the DSHB by Frankel, J. / Nelsen, E.M. (DSHB Hybridoma Product 12G10 anti-alpha-tubulin). Anti-SGK1 Rabbit IgG (Cell Signaling Technology, Cat # D27C11, #12103, Davers, MA).

Mice and Metabolic Experiments

C57Bl/6 two month old male mice (obtained from Charles River Laboratories, Wilmington , MA) were fed in their home cage with standard diet (0.25% sodium). Half the mice were then switched to a low salt diet (0.01-0.02% sodium, Sodium Deficient Diet, Harlan, Frederick, MD) for 3 days as described before(60). All animals were housed in the vivarium at Rangos Research Center at UPMC Children's Hospital of Pittsburgh, Pittsburgh, Pennsylvania, and all animal experiments were carried out in accordance with the policies of the Institutional Animal Care and Use Committee at the University of Pittsburgh.

Cell Culture

The mCCD-cl1 cells (kindly provided by B. Rossier and L. Schild, Université de Lausanne, Lausanne, Switzerland) were grown in flasks (passages 30–40) in defined (supplemented) medium at 37°C in 5% CO_2 as described previously(60, 61). The medium was changed every second day. For electrophysiological experiments, the mCCD cells were subcultured onto permeable filter supports (0.4 μm pore size, 0.33 cm^2 or 4 cm^2 surface area; Transwell, Corning, Lowell, MA). Typically, 24 hrs before use in any investigation, medium incubating

filter-grown cells were replaced with a minimal medium (without drugs or hormones) that contained DMEM and Ham F12 only. HEK-293 cells (from ATCC) were grown in flasks in DMEM (Invitrogen) supplemented with 10% FCS.

Plasmid Construction

The 3' UTRs of mouse MR and SGK1 were constructed using Gibson assembly of synthesized gene fragments (Integrated DNA Technologies, Coralville, IA) from the known sequences downloaded from the National Center for Biotechnology Information (NCBI) databases. For SGK1 we used GenBank Accession # NM_001161850 and MR (NR3C2) GenBank Accession # NM_001083906. The MR-UTR construct was engineered with AccI/SbfI and the SGK1-UTR with XhoI/XbaI restriction sequences for incorporation into a digested pMir-Glo dual luciferase reporter plasmid (Promega, Madison, WI). The putative miR-466 binding sites, located at positions 456 and 699 bp away from the termination codon in the MR-UTR and, 868 bp in the SGK1-UTR (see Fig.2) were eliminated and gene fragments assembled (as above) to produce UTRs in which the predicted miR-466 sites were absent. All constructs were sequenced (GeneWiz, South Plainfield, NJ) to verify the correct sequence and desired deletions were incorporated.

Short-Circuit Current Recordings and Equivalent Current Measurements

Inserts were mounted in modified Ussing chambers (P2300; Physiologic Instruments, San Diego, CA) and continuously short circuited with an automatic voltage clamp (VCC MC8; Physiologic Instruments) as described previously(60-62). The apical and basolateral chambers each contained 4 ml of Ringer solution (120 mM NaCl, 25 mM $NaHCO_3$, 3.3 mM KH_2PO_4, 0.8 mM K_2HPO_4, 1.2 mM $MgCl_2$, 1.2 mM $CaCl_2$, and 10 mM glucose). Chambers were constantly gassed with a mixture of 95% O_2, 5% CO_2 at 37°C, which maintained the pH at 7.4 and established a circulating perfusion bath within the Ussing chamber. Simultaneous transepithelial resistance was recorded by applying a 2-mV pulse per minute via an automated pulse generator. Recordings were digitized and analyzed using PowerLab (AD Instruments, Colorado Springs, CO). To screen for aldosterone-regulated miRs from mCCD-cl1 cells in culture, equivalent open circuit currents were obtained from cells using chopstick electrodes and an Epithelial Volt/Ohm Meter (EVOM) (World Precision Instruments, Sarasota, FL). Currents were calculated from cells stimulated with or without 50nM aldosterone for 24 hrs using Ohm's Law from the EVOM-measured open circuit voltages and transepithelial resistance.

Transfections: RNA Interference, miRNA Overexpression, and Depletion

DNA plasmids and RNA oligonucleotide constructs were transiently transfected into the mCCD and HEK293 cells using Lipofectamine 2000 (Invitrogen) according to the manufacturer's instructions and as described previously(60-62). The sequences for siRNA and all primers are listed in Table 1. Double-stranded RNA miR mimics (miRIDIAN microRNA Mimics) were obtained from Thermo Fisher Scientific. To inhibit processing to mature miRs and reduce endogenous miR expression, miRNA inhibitors, antisense modified RNA oligonucleotides (antagomirs), along with non-targeting miRNA inhibitor controls were obtained from IDT (Woburn, MA). Quantitative RT-PCR (below) was used to confirm miR overexpression or inhibition. For all transfections, mCCD cells were seeded onto 6-well

culture dishes at low density (~40%) and transfected with the chosen construct using Lipofectamine 2000. The cells remained in OptiMEM with the Lipofectamine 2000 overnight. The next day, cells were washed, lifted from the 6-well plates and seeded at super-density onto Transwell filters in fully supplemented medium. After 24 hrs during which time the cells attached to the filter supports, the cells were washed and placed in a minimal medium that contained only DMEM/F12 without additional supplementation (24 hrs) in preparation for aldosterone stimulation. Cells were then stimulated with aldosterone for the indicated times. Therefore, at the earliest stimulation timepoint (24-hour aldosterone) cells had been transfected for 96 hrs, and were on filters for 72 hrs.

Dual Luciferase Assays

HEK cells were transfected with pMIR-Glo containing MR and SGK1 wt or mutant 3' UTRs with or without miR-466 mimics. The following day the cells were sub-cultured to a white 96-well plate (Falcon, Thermo Fisher) and returned to the incubator. After 24 hours, luciferase activity was determined using the Dual-Glo Luciferase Assay System (Promega, Madison, WI) according to the manufacturer's protocol. Bioluminescence activity was recorded as an endpoint assay on a Synergy 1H plate reader (BioTek Instruments, Winooski, VT), with an integration time of 100ms at a sensitivity of 200.

RNA Isolation and qRT-PCR

RNA from cultured or primary CCD cells was isolated using the miRNeasy RNA isolation kit (Qiagen, Germantown, MD) according to the manufacturer's protocol. The kit facilitated isolation of both miRNA and total RNA from each sample for use in qRT-PCR and RT-PCR. Total RNA (containing miRNAs) concentration and quality were evaluated for inclusion in subsequent in vitro transcription assays based on a spectrophotometric absorption ratio of 260/280 >1.8 (NanoDrop, Wilmington, DE). Primers and primer pairs used for all PCRs are listed in Table 1. For qRT-PCR of miRNA, EvaGreen with ROX (MidSci, St Louis, MO) mastermix was used. For all miRNA qPCRs, the miRNA-specific forward primers were paired to a universal reverse primer as described before(60, 62). Real-time PCR was carried out using an Applied Biosystems 7900HT Fast Real-Time PCR System (Applied Biosystems, Life Technologies, Grand Island, NY). Detected signals from miR amplifications were normalized to the relative expression of small nucleolar RNA (SNO-202 and SNO-135) with each reaction/sample run in triplicate. Negative controls included no template and no primer omissions. The standard qPCR protocol is provided in Table 1. For qPCR of mRNA, primer pairs were used as listed (Table 1). Relative mRNA was normalized to the glyceraldehyde 3-phosphate dehydrogenase or actin message from each sample, and expression is presented as a fold change from control untreated samples (ΔΔCT).

Ex Vivo Kidney CCD Cell Isolation

Distal kidney nephron principal epithelial cells were isolated from a crude kidney tubule preparation (1 kidney from each animal) using a lectin binding and magnetic bead isolation technique as described before(60, 62). The isolated cells were immediately processed for RNA isolation; isolated RNA was used immediately or stored at −80°C until needed.

Western Blot

Lysates were prepared in cell lysis buffer (0.4% deoxycholic acid, 1% Nonidet P-40, 50 mM EGTA, 10 mM Tris-Cl, pH 7.4) plus protease inhibitors at 4°C for 10 min. The lysates were heated to 70°C for 5 min, separated by SDS-PAGE, transferred to Immobilon-P (EMD Millipore) and subjected to Western blot analysis using antibodies as indicated.

Blot Quantification and Statistical Analyses

Densitometric quantification of protein band intensities was carried out in Adobe Photoshop CS5.1 (Adobe Systems, Inc., San Jose, CA), and values were expressed as a percentage or fold change of control (unstimulated) signal, following background subtraction, and normalization to total protein expression (tubulin). Statistical analyses were performed using GraphPad Prism (Systat, La Jolla, CA). All data are presented as mean ± SEM. Repeats are defined as “N” for biological replicate and “n” for individual observations/samples. Data sets to be compared were tested for equal variance, and comparisons were performed using Mann–Whitney rank-sum and one-way ANOVA (multiple comparison) tests. Groups were considered statistically significant different at $p<0.05$. Significance is denoted by *** or ### = $p<0.001$, ** or ## = $p<0.01$, * or # = $p<0.05$.

Results

Aldosterone regulates miRs that target MR

To determine if the mouse MR 3’-UTR was targeted by aldosterone-regulated miRs, target prediction algorithms (miRDB and DianaTools) were used to rank potential MR binding miRs (Table 2)(63). Approximately 30 of the top ranked miRs were tested by qRT-PCR to determine if their expression was increased by aldosterone (50nM, 24hrs) in a mouse cortical collecting duct (mCCD) cell line. Total RNA from mCCD cells grown on filters was collected after a >50% increase in equivalent current aldosterone stimulation was observed (as measured using chopstick electrodes, data not shown). Of the tested miRs an increase in expression was observed for several miRs including mmu-miR-19a and mmu-miRs-466a/b/c/e-3p. The miR-466 family members represent a larger cluster of miRs in genomic proximity which include the miR-466, miR-467 and miR-669 family members. However, the miR-467 and −669 members that were tested did not exhibit elevated expression after 24hr aldosterone stimulation and were not further evaluated. The mature miRs-466a/b/c/d/e are nearly identical in mature sequence, with either the deletion of a single nucleotide at the beginning of the sequence (miRs-466b/c) or the omission of two nucleotides at the end of the sequence (miR-466d, Fig1A). While the precursor miR sequences differ, mature miR-466a&e and miR-466b&c sequences are identical. Consequently, results for these miRs were grouped together as miR-466a/e and miR-466b/c, as primers used in qRT-PCR analysis would be unable to distinguish between these mature forms. Target site predictions based on the seed sequence, identify the same targets for miR-466a, b, c & e family members due to the identical seed sequences. We therefore chose to base these studies on the miR-466b sequence (for mimic and antagomir). A time-course of miR-466 expression following extended aldosterone stimulation was performed to verify the initial screen and determine if these miRs remained elevated with extended aldosterone stimulation. The relative expression of miRs-466a/e and miR-466b/c increased following

aldosterone stimulation and were significantly higher at 72 hrs of aldosterone stimulation (Fig.1B). Levels of miR-466d and control miR-10a were not significantly changed. To confirm that a similar up-regulation of the miR-466 family members occurred *in vivo*, wt male mice were placed on a sodium deficient diet for 3 days. Distal nephron epithelial cells were isolated from kidneys of mice on control and sodium-deficient diets following enzymatic digestion and magnetic bead isolation as we have described previously(60, 62). The abundance of miRs-466a/e and miR-466b/c from isolated CCD cells in mice on a 72-hour low sodium diet was significantly greater relative to mice on normal sodium diets (Fig.1C). Expression of control miR-10a which is abundant in the CCD epithelial cells, and not regulated by aldosterone, related family member miR-466d and unrelated miR-466g were not significantly altered in response to the low Na^+ diet. To verify aldosterone stimulation in the *ex-vivo* isolated CCD cells, relative mRNA levels of SGK1, MR and αENaC were determined using qRT-PCR from mRNA isolated from in mice on low Na^+ diets compared to CCD cells isolated from mice on normal Na^+ diets (Fig.1D). SGK1 and αENaC mRNA levels were significantly greater in CCD cells isolated from the mice on low Na^+ diets compared to control diets.

miR-466 binds to the MR 3'-UTR

To confirm that miR-466 could bind the predicted target sequence on the 3'-UTR of MR (Fig.2A), a wt-UTR mouse MR or a MR-UTR with the miR-466 binding sites eliminated (MR-mutant) was inserted into a dual luciferase reporter construct. The reporter construct was co-transfected into HEK293 cells with a scrambled control or miR-466b mimic (50nM) and the luciferase signal measured (Fig.2B). Compared to the non-targeting control RNA, miR-466 mimics decreased the relative (normalized) luciferase signal by ~50%. The repression of the luciferase signal was not observed in the MR-mutant reporter where the predicted miR-466 binding sites were eliminated (Fig.2B).

SGK1 is targeted by miR-466

We examined the predicted miR binding sites of other known aldosterone-regulated proteins or components of the RAAS pathway. In mouse, SGK1, SGK3 and the angiotensin converting enzyme (ACE2) were predicted to be targeted by miR-466. As SGK1 is induced by aldosterone and alters Na^+ transport (via ENaC and other sodium transporters like NCC) in the mCCD cells, we investigated whether miR-466 regulated SGK1 expression. A dual-luciferase reporter was constructed with the 3'-UTR of SGK1 which has one predicted miR-466 target site (Fig.2C). As observed for MR, transfection of a miR-466 mimic significantly decreased the luciferase reporter signal. This inhibition was reversed when the miR-466 binding site was eliminated (Fig.2D). These reporter assays indicated that miR-466 was likely targeting both MR and SGK1 mRNA expression in the mCCD cells.

miR-466 alters MR and SGK protein expression

Binding of miR-466 in a reporter system may not translate to an alteration in final protein expression. As miR mimic overexpression could overload the endogenous RNA Induced Silencing Complex (RISC) protein machinery and produce an off-target phenotype by altering the expression of endogenous miRs, we chose to investigate the physiological impacts of miR-466 by using a miR-466 inhibitor (antagomir). This inhibitor was successful

in significantly reducing the expression of endogenous miR-466a/e & b/c without impacting non-targeted miRs (miR-10a for example, Fig.3A). The longevity of antagomir action was determined by obtaining RNA from cells 24-96 hrs after transfection and determining relative miR-466 abundance compared to control transfected mCCD cells. Relative expression of the targeted miR-466a/e,b/c remained significantly repressed at 96 hrs (Fig.3B) compared to controls. Cells were next transfected with the miR-466 antagomir, seeded onto filters and stimulated with aldosterone for 24, 48 and 72hrs hours. The reduction in miR-466 resulted in an increase of MR protein expression (Fig.3C). Previous reports of aldosterone stimulation noted MR protein modification (ubiquitination, acetylation and phosphorylation) and the reduction in protein expression. In line with these previous reports, we note that there is a shift in the apparent molecular weight of MR after aldosterone stimulation in mCCD cells (Fig.3C). By introducing the miR-466 inhibitor the protein expression in the presence of aldosterone was significantly greater compared to cells transfected with a non-targeting control (Fig.3D).

Aldosterone stimulation significantly increased SGK1 expression (Fig. 3C). The level of SGK1 before aldo stimulation is very low and not significantly increased by miR-466 inhibition. Under unstimulated conditions, miR-466 expression has a minimal impact on SGK1 levels, as both miR and target are expressed at relatively low levels. Stimulation with aldosterone (50nM for 24-72 hrs) causes an increase in SGK1 expression that was significantly greater when miR-466 was inhibited (Fig.3E). Therefore, as SGK1 levels are rising, miR-466 is up-regulated and this reduces the final protein levels of SGK1. By inhibiting miR-466 the repressed SGK1 protein levels are further increased.

Aldosterone-stimulated Na^+ transport is increased with miR-466 inhibition

To determine if the relative increase in MR and SGK1 protein levels with miR-466 inhibition results in an increase in Na^+ transport with aldosterone stimulation, mCCD cells were transfected with the miR-466 inhibitor and stimulated with aldosterone. As shown in Fig. 4A a significant increase in ENaC-mediated Na^+ transport was observed in miR-466 inhibited cells after a 24-hour aldosterone stimulation compared to control transfected cells (Fig.4 A). Baseline (unstimulated) amiloride-sensitive ENaC currents are not different. Previous studies examining extended aldosterone stimulation have noted that the initial increase in ENaC-mediated Na^+ transport observed following aldosterone stimulation gradually falls back to baseline in the presence of extended aldosterone stimulation. A similar trend was observed in control mCCD cells with a 72-hour aldosterone stimulation (Fig.4B). Absolute amiloride-sensitive current was maximal after a 24-hour stimulation and returned close to baseline after 72 hrs of continued aldosterone stimulation. In cells overexpressing the miR-466 inhibitor, two differences were observed. First the magnitude of the aldosterone stimulation was higher, and the decline in stimulated transport was reduced. ENaC-mediated Na^+ transport remained elevated over the 72-hour time-course. When measured currents were normalized and expressed as a percentage of unstimulated currents for cells recorded on the same day (same transfection), the miR-466 inhibitor overexpressing cells had a significantly greater current compared to control cells after 72 hrs (Fig.4C) and the decline in current was not apparent. By inhibiting the aldosterone-induced increase in miR-466 expression, the ability of these miRs to bind to their validated MR and SGK1

targets was prevented, resulting in elevated and sustained responses to extended aldosterone stimulation.

To examine if the elevated miR-466 was acting as a repressor of aldosterone signaling, mCCD cells overexpressing the miR-466 inhibitor were stimulated with an aldosterone dose response (for 24 hrs). Representative current traces from mCCD cells mounted in Ussing chambers from control and miR-466 inhibited cells are presented in Fig.5A. Summarized data were normalized to the control unstimulated ENaC currents for each day of recording and the ENaC-mediated current response plotted (Fig.5B). Both the sensitivity to and magnitude of the aldosterone stimulation was increased in cells where miR-466 was inhibited. The calculated EC_{50} for aldosterone response is indicated next to each fitted curve

RAAS proteins share predicted miR binding sites

By identifying RAAS components all targeted by the same miRs, we evaluated the network of miRs predicted to bind to RAAS mRNAs. We constructed a prediction heatmap that included known RAAS proteins and channels/transporters and proteins involved in Na^+ reabsorption in the kidney distal nephron (Fig.6). The matrix represents the percentage of miRs predicted to bind to their target that are predicted to bind to other RAAS mRNAs. In some cases, we found that as many as 40% of the predicted miRs are shared between targets. Therefore, if a set of miRs are up-regulated in response to aldosterone, these miRs would have the ability to simultaneously target several components of RAAS signaling. This would provide a mechanism for feedback regulation of RAAS signaling with extended aldosterone stimulation. For example, another of the up-regulated miRs that targeted MR was miR-19a. MiR-19 is predicted to bind SGK1, ATP1B4, ACE2, AGTR1B in mouse and WNK1, ATP1A2, MR, SGK1 in humans.

Discussion

Our previous studies detailed the increase in miR expression in CCD cells after aldosterone stimulation. In those studies, a single timepoint and dose of aldosterone was considered(60, 62). The results supported the role of miR regulation by aldosterone. The targets of the upregulated miRs included proteins involved in regulating the trafficking of ion channels from the apical surface of epithelial cells of the distal nephron(62, 64). By decreasing the expression of these target proteins, channel internalization was reduced, resulting in an increase in Na^+ and K^+ transport, consistent with the role of aldosterone signaling in the kidney. The studies presented here however, investigate an extended aldosterone response.

Elevated aldosterone levels or defective signaling in the RAAS cascade are linked to an increased risk of stroke, atrial fibrillation, diabetes, increased blood pressure, cardiac remodeling, cardiac hypertrophy, cardiac fibrosis and arterial stiffening(65-77). Homeostatic regulation of Na^+ transport must therefore balance the need to restore plasma Na^+ levels with the risk of cellular damage induced by exposure to aldosterone for days (or longer). Cellular sensitivity to aldosterone is known to decrease with extended exposure. This can be attributed in part to downregulation of the MR which occurs after binding to aldosterone(19, 78, 79). The downregulation of MR occurs at the level of both protein and mRNA(19). Negative feedback of MR reduces aldosterone signaling in cells and this is often observed in

cultured cells as the ENaC-mediated aldosterone response plateaus after an initial increase in the first 24 hrs (see Figure 4C). The observation that MR mRNA expression was decreased in mice placed on extended (7-day) low Na^+ diets to induce aldosterone signaling, suggested the possibility of a post-transcriptional regulation of the MR mRNA(19). This is one of the best characterized functions of miRs(45, 80, 81), and prompted the investigation into long-term aldosterone induction of miRs in the distal nephron epithelial cells. By profiling the miRs predicted to bind to the 3'-UTR of mouse MR, we identified several miRs that were upregulated by aldosterone, that had not been previously investigated. While some of these were noted in the microarray analysis in our previous studies(60), the miR-466 family members were not evaluated before because their baseline (unstimulated) expression fell below our threshold for inclusion. Nevertheless, this cluster has been studied in mice and shown to play a role in osmoregulation in the kidney(82). Another miR-466 isoform (not part of this cluster), miR-466g was also shown to target SGK1(83).

As miRs-466a/e & b/c were upregulated after a 24-hour aldosterone stimulation, our focus shifted to the miR-466 family. The upregulation of miR-466 persisted while the cells remained aldosterone stimulated, and expression was greater at 72 hrs than 24 hrs. A similar (and more pronounced) upregulation of miR-466 was observed *in vivo* in CCD cells isolated from mouse kidneys in animals on low Na^+ diets (for 72 hrs). It should be noted that the levels of miR-466 in unstimulated cells begins at a low level. Upon aldosterone stimulation, the miR-466 family members increase expression, so that when normalized to the starting levels this fold increase *in vivo* appears large. After extended aldosterone exposure, the miR levels rise and mCCD cells gradually decrease the positive regulators of Na^+ transport to damp down the aldosterone signal. This is evident in experiments where the increase in endogenous miR-466 is prevented using an antagomir. Unstimulated ENaC transport is not significantly different in miR-466 inhibited cells compared to controls. However, once the cells are stimulated with aldosterone the inhibitory impact of the miR-466 family is evident. When these miRs are prevented from feeding back to inhibit MR and SGK1 mRNAs the final protein expression is increased and the Na^+ currents are significantly higher. Desensitization of mCCD cells to extended aldosterone stimulation in control cells is evident as a fall in stimulated ENaC currents over time (>24 hrs), and this decline was not observed in miR-466 inhibited cells. The elevated ENaC transport persisted for 72 hrs.

Our previous studies characterized miRs that are upregulated and downregulated by aldosterone. In both cases, the investigated target of the regulated miRs were proteins associated with trafficking of sodium transporters to the apical surface. In the case of the downregulated miRs, the target mRNA, Ank3 facilitated delivery of ENaC to the apical surface of mCCD cells(60). Upregulation of this protein increased ENaC traffic to the surface. Conversely, the upregulated miRs targeted the clathrin-binding protein intersectin 2. By inhibiting this target, ENaC surface residency was increased. In both cases the net result was an increase in ENaC at the apical surface, one of the known actions of aldosterone. However, in both these studies, a single 24-hour timepoint was investigated. In this work we add to the list of miRs regulated by aldosterone and demonstrate that over a longer aldosterone stimulation, expression of many of the miR-466 family members is increased. These miRs can target MR and SGK1, and likely form part of an extended miR-mRNA interactome that fine-tunes RAAS signaling.

In conclusion, we demonstrate a novel component in the RAAS signaling cascade that would control sodium homeostasis. MiRs activated following extended aldosterone stimulation serve as negative feedback regulators in renal epithelial cells to reduce components of the signaling cascade over time. It is likely that additional miRs are involved in this long-term regulation, and possible that the same miRs may downregulate RAAS proteins further upstream in the cascade. The role of miRs should therefore be considered to gain a full understanding of kidney sodium homeostasis.

Acknowledgements

Funding for the research was provided to MBB from the NIH NIDDK DK102843 and to JH from NIDDK DK103776.

Abbreviations

ACE2	Angiotensin-converting enzyme 2
AGTR1B	Angiotensin II receptor, type 1b
ATP1A2	ATPase, Na^+/K^+ transporting, alpha 2 polypeptide
ATP1B4	ATPase Na+/K+ Transporting Family Member Beta 4
miRs	microRNAs
MR	Mineralocorticoid Receptor
NCC	Sodium-chloride co-transporter (SLC12A3)
SGK1	Serum and Glucocorticoid induced Kinase 1
WNK1	WNK Lysine Deficient Protein Kinase 1

References

1. Tomaschitz A, Pilz S, Ritz E, Obermayer-Pietsch B, and Pieber TR (2010) Aldosterone and arterial hypertension. Nat. Rev. Endocrinol 6, 83–93 [PubMed: 20027193]
2. Sowers JR, Whaley-Connell A, and Epstein M (2009) Narrative review: the emerging clinical implications of the role of aldosterone in the metabolic syndrome and resistant hypertension. Ann. Intern. Med 150, 776–783 [PubMed: 19487712]
3. Rossi GP, Sechi LA, Giacchetti G, Ronconi V, Strazzullo P, and Funder JW (2008) Primary aldosteronism: cardiovascular, renal and metabolic implications. Trends Endocrinol. Metab 19, 88–90 [PubMed: 18314347]
4. Komukai K, Mochizuki S, and Yoshimura M (2010) Gender and the renin-angiotensin-aldosterone system. Fund. Clin. Pharmacol 24, 687–698
5. Jansen PM, Danser AH, Imholz BP, and van den Meiracker AH (2009) Aldosterone-receptor antagonism in hypertension. J. Hypertens 27, 680–691 [PubMed: 19516169]
6. Engeli S (2006) Role of the renin-angiotensin- aldosterone system in the metabolic syndrome. Contrib. Nephrol 151, 122–134 [PubMed: 16929137]
7. Lakkis J, Lu WX, and Weir MR (2003) RAAS escape: a real clinical entity that may be important in the progression of cardiovascular and renal disease. Curr. Hypertens. Rep 5, 408–417 [PubMed: 12948434]

8. Willenberg HS, Schinner S, and Ansurudeen I (2008) New mechanisms to control aldosterone synthesis. Horm. Metab. Res 40, 435–441 [PubMed: 18493881]
9. Hattangady NG, Olala LO, Bollag WB, and Rainey WE (2012) Acute and chronic regulation of aldosterone production. Mol. Cell. Endocrinol 350, 151–162 [PubMed: 21839803]
10. Nogueira EF, Bollag WB, and Rainey WE (2009) Angiotensin II regulation of adrenocortical gene transcription. Mol. Cell. Endocrinol 302, 230–236 [PubMed: 18812209]
11. Spat A, and Hunyady L (2004) Control of aldosterone secretion: a model for convergence in cellular signaling pathways. Physiol. Rev 84, 489–539 [PubMed: 15044681]
12. Berger S, Bleich M, Schmid W, Greger R, and Schutz G (2000) Mineralocorticoid receptor knockout mice: lessons on Na^+ metabolism. Kidney Int. 57, 1295–1298 [PubMed: 10760057]
13. Fejes-Toth G, Pearce D, and Naray-Fejes-Toth A (1998) Subcellular localization of mineralocorticoid receptor in living cells: effects of receptor agonist and antagonists. PNAS 95, 2973–2978 [PubMed: 9501200]
14. Strazzullo P, Galletti F, and Barba G (2003) Altered renal handling of sodium in human hypertension: short review of the evidence. Hypertension 41, 1000–1005 [PubMed: 12668589]
15. Meneton P (2000) Comparative roles of the renal apical sodium transport systems in blood pressure control. J. Am. Soc. Nephrol 11 Suppl 16, S135–139 [PubMed: 11065345]
16. Antes LM, Kujubu DA, and Fernandez PC (1998) Hypokalemia and the pathology of ion transport molecules. Semin. Nephrol 18, 31–45 [PubMed: 9459287]
17. Shibata S, Rinehart J, Zhang J, Moeckel G, Castaneda-Bueno M, Stiegler AL, Boggon TJ, Gamba G, and Lifton RP (2013) Mineralocorticoid receptor phosphorylation regulates ligand binding and renal response to volume depletion and hyperkalemia. Cell Metab. 18, 660–671 [PubMed: 24206662]
18. Faresse N, Vitagliano JJ, and Staub O (2012) Differential ubiquitylation of the mineralocorticoid receptor is regulated by phosphorylation. FASEB J. 26, 4373–4382 [PubMed: 22798426]
19. Poulsen SB, Limbutara K, Fenton RA, Pisitkun T, and Christensen BM (2018) RNA sequencing of kidney distal tubule cells reveals multiple mediators of chronic aldosterone action. Physiol. Genomics 50, 343–354 [PubMed: 29521601]
20. Vallon V, Wulff P, Huang DY, Loffing J, Volkl H, Kuhl D, and Lang F (2005) Role of Sgk1 in salt and potassium homeostasis. Am. J. Physiol. Regul. Integr. Comp. Physiol 288, R4–10 [PubMed: 15590995]
21. Verrey F, Loffing J, Zecevic M, Heitzmann D, and Staub O (2003) SGK1: aldosterone-induced relay of Na^+ transport regulation in distal kidney nephron cells. Cell. Physiol. Biochem 13, 21–28 [PubMed: 12649599]
22. Wulff P, Vallon V, Huang DY, Volkl H, Yu F, Richter K, Jansen M, Schlunz M, Klingel K, Loffing J, Kauselmann G, Bosl MR, Lang F, and Kuhl D (2002) Impaired renal Na(+) retention in the sgk1-knockout mouse. J. Clin. Invest 110, 1263–1268 [PubMed: 12417564]
23. Debonneville C, Flores SY, Kamynina E, Plant PJ, Tauxe C, Thomas MA, Munster C, Chraibi A, Pratt JH, Horisberger JD, Pearce D, Loffing J, and Staub O (2001) Phosphorylation of Nedd4-2 by Sgk1 regulates epithelial Na(+) channel cell surface expression. EMBO J. 20, 7052–7059 [PubMed: 11742982]
24. de Seigneux S, Leroy V, Ghzili H, Rousselot M, Nielsen S, Rossier BC, Martin PY, and Feraille E (2008) NF-kappaB inhibits sodium transport via down-regulation of SGK1 in renal collecting duct principal cells. J. Biol. Chem 283, 25671–25681 [PubMed: 18586672]
25. Rayner B (2008) Primary aldosteronism and aldosterone-associated hypertension. J. Clin. Pathol 61, 825–831 [PubMed: 18587013]
26. Verrey F, Pearce D, Pfeiffer R, Spindler B, Mastroberardino L, Summa V, and Zecevic M (2000) Pleiotropic action of aldosterone in epithelia mediated by transcription and post-transcription mechanisms. Kidney Int. 57, 1277–1282 [PubMed: 10760054]
27. Ouar Z, Sole E, Bens M, Rafestin-Oblin ME, Meseguer A, and Vandewalle A (1998) Pleiotropic effects of dihydrotestosterone in immortalized mouse proximal tubule cells. Technical note. Kidney Int 53, 59–66 [PubMed: 9453000]
28. He L, and Hannon GJ (2004) MicroRNAs: small RNAs with a big role in gene regulation. Nat. Rev. Genet 5, 522–531 [PubMed: 15211354]

29. Lim LP, Glasner ME, Yekta S, Burge CB, and Bartel DP (2003) Vertebrate microRNA genes. Science 299, 1540 [PubMed: 12624257]
30. Grad Y, Aach J, Hayes GD, Reinhart BJ, Church GM, Ruvkun G, and Kim J (2003) Computational and experimental identification of C. elegans microRNAs. Mol. Cell 11, 1253–1263 [PubMed: 12769849]
31. Lee Y, Jeon K, Lee JT, Kim S, and Kim VN (2002) MicroRNA maturation: stepwise processing and subcellular localization. EMBO J. 21, 4663–4670 [PubMed: 12198168]
32. Lau NC, Lim LP, Weinstein EG, and Bartel DP (2001) An abundant class of tiny RNAs with probable regulatory roles in Caenorhabditis elegans. Science 294, 858–862 [PubMed: 11679671]
33. Ha M, and Kim VN (2014) Regulation of microRNA biogenesis. Nat. Rev. Mol. Cell. Biol 15, 509–524 [PubMed: 25027649]
34. Breving K, and Esquela-Kerscher A (2010) The complexities of microRNA regulation: mirandering around the rules. Int. J. Biochem. Cell Biol 42, 1316–1329 [PubMed: 19800023]
35. Chua JH, Armugam A, and Jeyaseelan K (2009) MicroRNAs: biogenesis, function and applications. Curr. Opin. Mol. Ther 11, 189–199 [PubMed: 19330724]
36. Winter J, Jung S, Keller S, Gregory RI, and Diederichs S (2009) Many roads to maturity: microRNA biogenesis pathways and their regulation. Nat. Cell Biol 11, 228–234 [PubMed: 19255566]
37. Butterworth MB, and Alvarez de la Rosa D (2019) Regulation of Aldosterone Signaling by MicroRNAs. Vitam. Horm 109, 69–103 [PubMed: 30678867]
38. Butterworth MB (2015) MicroRNAs and the regulation of aldosterone signaling in the kidney. Am. J. Physiol. Cell Physiol 308, C521–527 [PubMed: 25673770]
39. Batkai S, and Thum T (2012) MicroRNAs in hypertension: mechanisms and therapeutic targets. Curr. Hypertens. Rep 14, 79–87 [PubMed: 22052337]
40. Kim YK, and Kim VN (2007) Processing of intronic microRNAs. EMBO J. 26, 775–783 [PubMed: 17255951]
41. Jiang F, Ye X, Liu X, Fincher L, McKearin D, and Liu Q (2005) Dicer-1 and R3D1-L catalyze microRNA maturation in Drosophila. Gene. Dev 19, 1674–1679 [PubMed: 15985611]
42. Lee YS, Nakahara K, Pham JW, Kim K, He Z, Sontheimer EJ, and Carthew RW (2004) Distinct roles for Drosophila Dicer-1 and Dicer-2 in the siRNA/miRNA silencing pathways. Cell 117, 69–81 [PubMed: 15066283]
43. Han J, Lee Y, Yeom KH, Kim YK, Jin H, and Kim VN (2004) The Drosha-DGCR8 complex in primary microRNA processing. Gene. Dev 18, 3016–3027 [PubMed: 15574589]
44. Lee Y, Ahn C, Han J, Choi H, Kim J, Yim J, Lee J, Provost P, Radmark O, Kim S, and Kim VN (2003) The nuclear RNase III Drosha initiates microRNA processing. Nature 425, 415–419 [PubMed: 14508493]
45. Liu X, Jin DY, McManus MT, and Mourelatos Z (2012) Precursor microRNA-programmed silencing complex assembly pathways in mammals. Mol. Cell 46, 507–517 [PubMed: 22503104]
46. Sontheimer EJ, and Carthew RW (2004) Molecular biology. Argonaute journeys into the heart of RISC. Science 305, 1409–1410 [PubMed: 15353786]
47. Okamura K, Ishizuka A, Siomi H, and Siomi MC (2004) Distinct roles for Argonaute proteins in small RNA-directed RNA cleavage pathways. Gene. Dev 18, 1655–1666 [PubMed: 15231716]
48. Jaskiewicz L, and Filipowicz W (2008) Role of Dicer in posttranscriptional RNA silencing. Curr. Top. Microbiol. Immunol 320, 77–97 [PubMed: 18268840]
49. Forstemann K, Horwich MD, Wee L, Tomari Y, and Zamore PD (2007) Drosophila microRNAs are sorted into functionally distinct argonaute complexes after production by dicer-1. Cell 130, 287–297 [PubMed: 17662943]
50. Tang G (2005) siRNA and miRNA: an insight into RISCs. Trends Biochem. Sci 30, 106–114 [PubMed: 15691656]
51. Kim VN (2005) Small RNAs: classification, biogenesis, and function. Mol. Cell 19, 1–15 [PubMed: 15989960]
52. Bartel DP (2004) MicroRNAs: genomics, biogenesis, mechanism, and function. Cell 116, 281–297 [PubMed: 14744438]

53. Lewis BP, Shih IH, Jones-Rhoades MW, Bartel DP, and Burge CB (2003) Prediction of mammalian microRNA targets. Cell 115, 787–798 [PubMed: 14697198]
54. Ilatovskaya DV, Levchenko V, Pavlov TS, Isaeva E, Klemens CA, Johnson J, Liu P, Kriegel AJ, and Staruschenko A (2019) Salt-deficient diet exacerbates cystogenesis in ARPKD via epithelial sodium channel (ENaC). EBioMedicine 40, 663–674 [PubMed: 30745171]
55. Butterworth MB (2018) Role of microRNAs in aldosterone signaling. Curr. Opin. Nephrol. Hypertens 27, 390–394 [PubMed: 30074910]
56. Parreira RC, Lacerda LHG, Vasconcellos R, Lima SS, Santos AK, Fontana V, Sandrim VC, and Resende RR (2017) Decoding resistant hypertension signalling pathways. Clin. Sci. (Lond) 131, 2813–2834 [PubMed: 29184046]
57. Pacurari M, and Tchounwou PB (2015) Role of MicroRNAs in Renin-Angiotensin-Aldosterone System-Mediated Cardiovascular Inflammation and Remodeling. Int. J. Inflam 2015, 101527 [PubMed: 26064773]
58. Chen LJ, Xu R, Yu HM, Chang Q, and Zhong JC (2015) The ACE2/Apelin Signaling, MicroRNAs, and Hypertension. Int. J. Hypertens 2015, 896861 [PubMed: 25815211]
59. Nossent AY, Hansen JL, Doggen C, Quax PH, Sheikh SP, and Rosendaal FR (2011) SNPs in microRNA binding sites in 3'-UTRs of RAAS genes influence arterial blood pressure and risk of myocardial infarction. Am. J. Hypertens 24, 999–1006 [PubMed: 21677697]
60. Edinger RS, Coronnello C, Bodnar AJ, Labarca M, Bhalla V, LaFramboise WA, Benos PV, Ho J, Johnson JP, and Butterworth MB (2014) Aldosterone regulates microRNAs in the cortical collecting duct to alter sodium transport. J. Am. Soc. Nephrol 25, 2445–2457 [PubMed: 24744440]
61. Edinger RS, Bertrand CA, Rondandino C, Apodaca GA, Johnson JP, and Butterworth MB (2012) The epithelial sodium channel (ENaC) establishes a trafficking vesicle pool responsible for its regulation. PloS one 7, e46593 [PubMed: 23029554]
62. Liu X, Edinger RS, Klemens CA, Phua YL, Bodnar AJ, LaFramboise WA, Ho J, and Butterworth MB (2017) A MicroRNA Cluster miR-23-24-27 Is Upregulated by Aldosterone in the Distal Kidney Nephron Where it Alters Sodium Transport. J. Cell Physiol 232, 1306–1317 [PubMed: 27636893]
63. Wong N, and Wang X (2015) miRDB: an online resource for microRNA target prediction and functional annotations. Nucleic Acids Res.43, D146–152 [PubMed: 25378301]
64. Lin DH, Yue P, Zhang C, and Wang WH (2014) MicroRNA-194 (miR-194) regulates ROMK channel activity by targeting intersectin 1. Am. J. Physiol. Renal Physiol 306, F53–60 [PubMed: 24197061]
65. Ohno Y, Sone M, Inagaki N, Yamasaki T, Ogawa O, Takeda Y, Kurihara I, Itoh H, Umakoshi H, Tsuiki M, Ichijo T, Katabami T, Tanaka Y, Wada N, Shibayama Y, Yoshimoto T, Ogawa Y, Kawashima J, Takahashi K, Fujita M, Watanabe M, Matsuda Y, Kobayashi H, Shibata H, Kamemura K, Otsuki M, Fujii Y, Yamamoto K, Ogo A, Okamura S, Miyauchi S, Fukuoka T, Izawa S, Yoneda T, Hashimoto S, Yanase T, Suzuki T, Kawamura T, Tabara Y, Matsuda F, Naruse M, Nagahama S, and Group JS (2018) Prevalence of Cardiovascular Disease and Its Risk Factors in Primary Aldosteronism: A Multicenter Study in Japan. Hypertension 71, 530–537 [PubMed: 29358460]
66. Monticone S, D'Ascenzo F, Moretti C, Williams TA, Veglio F, Gaita F, and Mulatero P (2018) Cardiovascular events and target organ damage in primary aldosteronism compared with essential hypertension: a systematic review and meta-analysis. Lancet Diabetes Endocrinol. 6, 41–50 [PubMed: 29129575]
67. Fitzgerald MA (2011) Hypertension treatment update: focus on direct renin inhibition. J. Am. Acad. Nurse Prac 23, 239–248
68. Vijayaraghavan K, and Deedwania P (2011) Renin-angiotensin-aldosterone blockade for cardiovascular disease prevention. Cardiol. Clin 29, 137–156 [PubMed: 21257105]
69. Chrysant SG (2010) The role of Angiotensin receptor blocker and calcium channel blocker combination therapy in treating hypertension: focus on recent studies. Am. J. Cardiovasc. Drugs 10, 315–320 [PubMed: 20860414]

70. Volpe M, McKelvie R, and Drexler H (2010) Hypertension as an underlying factor in heart failure with preserved ejection fraction. J. Clin. Hypertens. (Greenwich) 12, 277–283 [PubMed: 20433548]
71. Ismail H, Mitchell R, McFarlane SI, and Makaryus AN (2010) Pleiotropic effects of inhibitors of the RAAS in the diabetic population: above and beyond blood pressure lowering. Curr. Diabetes Rep. 10, 32–36
72. Papademetriou V (2009) Inhibition of the renin-angiotensin-aldosterone system to prevent ischemic and atherothrombotic events. Am. Heart J. 157, S24–30 [PubMed: 19450721]
73. Sciarretta S, Paneni F, Palano F, Chin D, Tocci G, Rubattu S, and Volpe M (2009) Role of the renin-angiotensin-aldosterone system and inflammatory processes in the development and progression of diastolic dysfunction. Clin. Sci. (Lond) 116, 467–477 [PubMed: 19200056]
74. Coccheri S (2007) Approaches to prevention of cardiovascular complications and events in diabetes mellitus. Drugs 67, 997–1026 [PubMed: 17488145]
75. Baluta M, Vintila V, and Vintila M (2004) Renin-Angiotensin-Aldosterone system inhibition in prevention of diabetes mellitus. Rom. J. Intern. Med 42, 277–288 [PubMed: 15529618]
76. Sokol SI, Portnay EL, Curtis JP, Nelson MA, Hebert PR, Setaro JF, and Foody JM (2004) Modulation of the renin-angiotensin-aldosterone system for the secondary prevention of stroke. Neurology 63, 208–213 [PubMed: 15277610]
77. Felmeden DC, and Lip GY (2000) The renin-angiotensin-aldosterone system and fibrinolysis. J. RENIN-ANGIO-ALDO S 1, 240–244
78. Lang F (2014) On the pleotropic actions of mineralocorticoids. Nephron Physiol. 128, 1–7 [PubMed: 25376771]
79. Briet M, and Schiffrin EL (2010) Aldosterone: effects on the kidney and cardiovascular system. Nat. Rev. Nephrol6, 261–273 [PubMed: 20234356]
80. Trionfini P, Benigni A, and Remuzzi G (2015) MicroRNAs in kidney physiology and disease. Nat. Rev. Nephrol 11, 23–33 [PubMed: 25385286]
81. Agarwal V, Bell GW, Nam JW, and Bartel DP (2015) Predicting effective microRNA target sites in mammalian mRNAs. eLife 4
82. Luo Y, Liu Y, Liu M, Wei J, Zhang Y, Hou J, Huang W, Wang T, Li X, He Y, Ding F, Yuan L, Cai J, Zheng F, and Yang JY (2014) Sfmbt2 10th intron-hosted miR-466(a/e)-3p are important epigenetic regulators of Nfat5 signaling, osmoregulation and urine concentration in mice. Biochim. Biophys. Acta 1839, 97–106 [PubMed: 24389345]
83. Jacobs ME, Kathpalia PP, Chen Y, Thomas SV, Noonan EJ, and Pao AC (2016) SGK1 Regulation by miR-466g in Cortical Collecting Duct Cells. Am. J. Physiol. Renal Physiol, 10(11):F1251–7

miR Name	Precursor sequence	Mature sequence	Mouse genomic location
mmu-miR-466a-3p	uauauguguuuauguguguguacauguacauaugug aauaugauauccauauacauacacgcacacauaagac	5' - uauacauacacgcacacauaaga - 3'	chr2:10507918-10507990 (+)
mmu-miR-466b-3p	uguauguguugaugugugugguacauguacaugucug aauaugauauacauauacauacacgcacacauaaga cacauaugag	5' - uauacauacacgcacacauaaga - 3'	chr2:10474219-10474300 (+)
mmu-miR-466c-3p	guauauguguugaugugugugugcauguacauaugu gaauaugauauacauauacauacacgcacacauaag acacauaugagc	5' - uauacauacacgcacacauaaga - 3'	chr2:10481534-10481617 (+)
mmu-miR-466d-3p	caugugugguuugugugugcguacauguacaugugug uauaugaauauacauauacauacacgcacacauaga uacgcacgcacacacacacacagg	5' – uauacauacacgcacacauaag - 3'	chr2:10511967-10512062 (+)
mmu-miR-466e-3p	guguauguguugaugugugugguacauguacauaugu gaauaugauauacauauacauacacgcacacauaag acacauaugagc	5' - uauacauacacgcacacauaaga - 3'	chr2:10479088-10479171 (+)

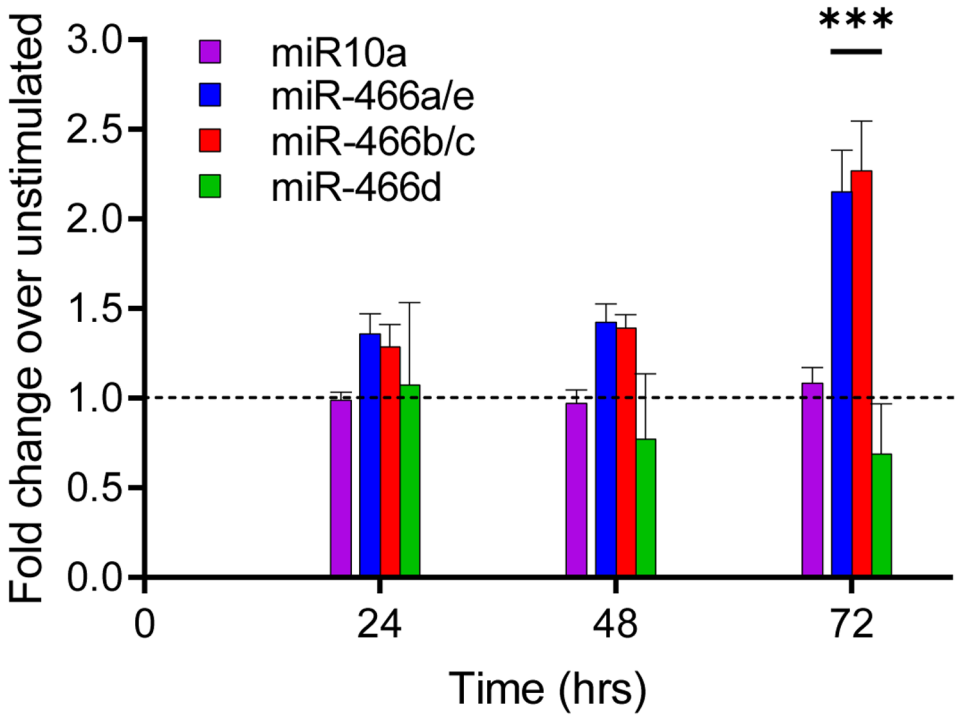

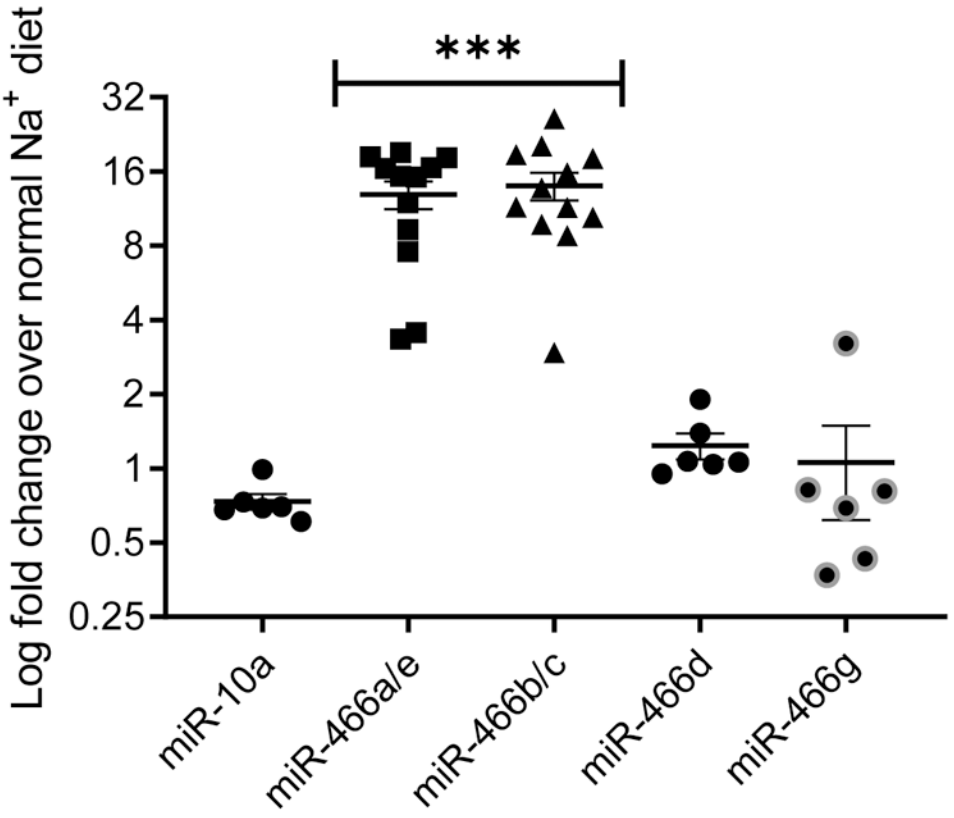

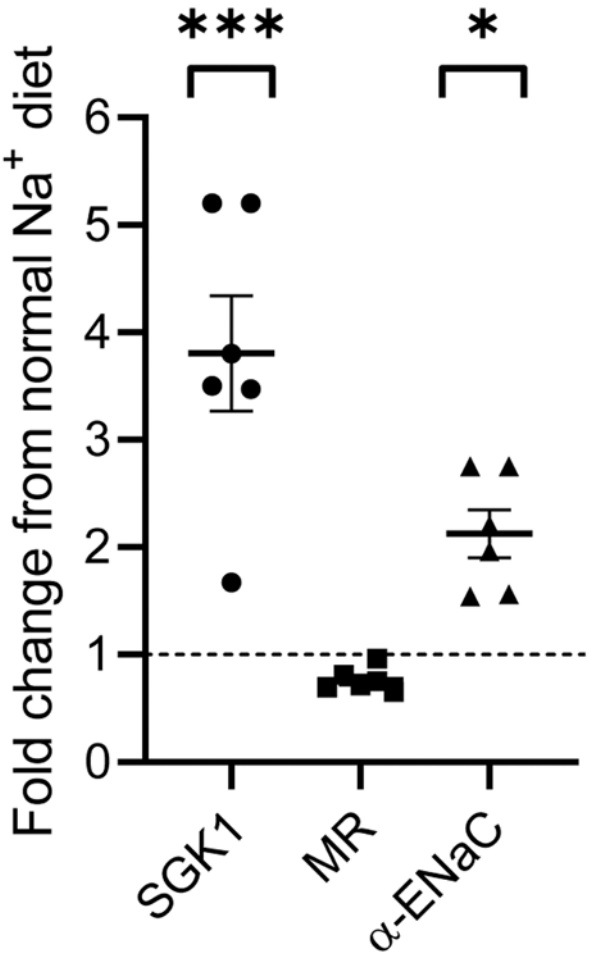

Figure 1:

A) The precursor and mature sequences of mouse miR-466 family members, with the genomic location of each are listed. The position of the mature miRs embedded in each precursor sequence is highlighted in blue text. Variations from the miR-466a sequence are highlighted with ▮ indicating deletions at the beginning of the sequence, or ▮ representing insertions/deletions within the sequence. Mature sequences of miRs-466 a & e and miRs-466 b & c are identical even though their precursor sequences differ. B) qRT-PCR determination of the relative expression of miRs-466 a/e, b/c, d and control miR-10a after aldosterone stimulation (50nM, 24-72 hrs) compared to unstimulated mCCD cells (N≥5, n=5-17 for each bar, *** $p<0.001$ compared to unstimulated, one-way ANOVA). C) Relative expression of miR-466 a/e, b/c, d, miR-10a (control) and a non-family member miR-466g in CCD cells isolated from mice on low Na^+ diets compared to miR expression on normal Na^+ diets (N=6, *** $p<0.001$, one-way ANOVA). D) Relative expression of SGK1, MR and αENaC mRNA from the same samples as in Fig.1C. Both SGK1 and aENaC expression was significantly greater in CCD cells isolated from mice on low Na^+ diet compared to control diet. (N=6, *** $p<0.001$, * $P<0.05$ one-way ANOVA).

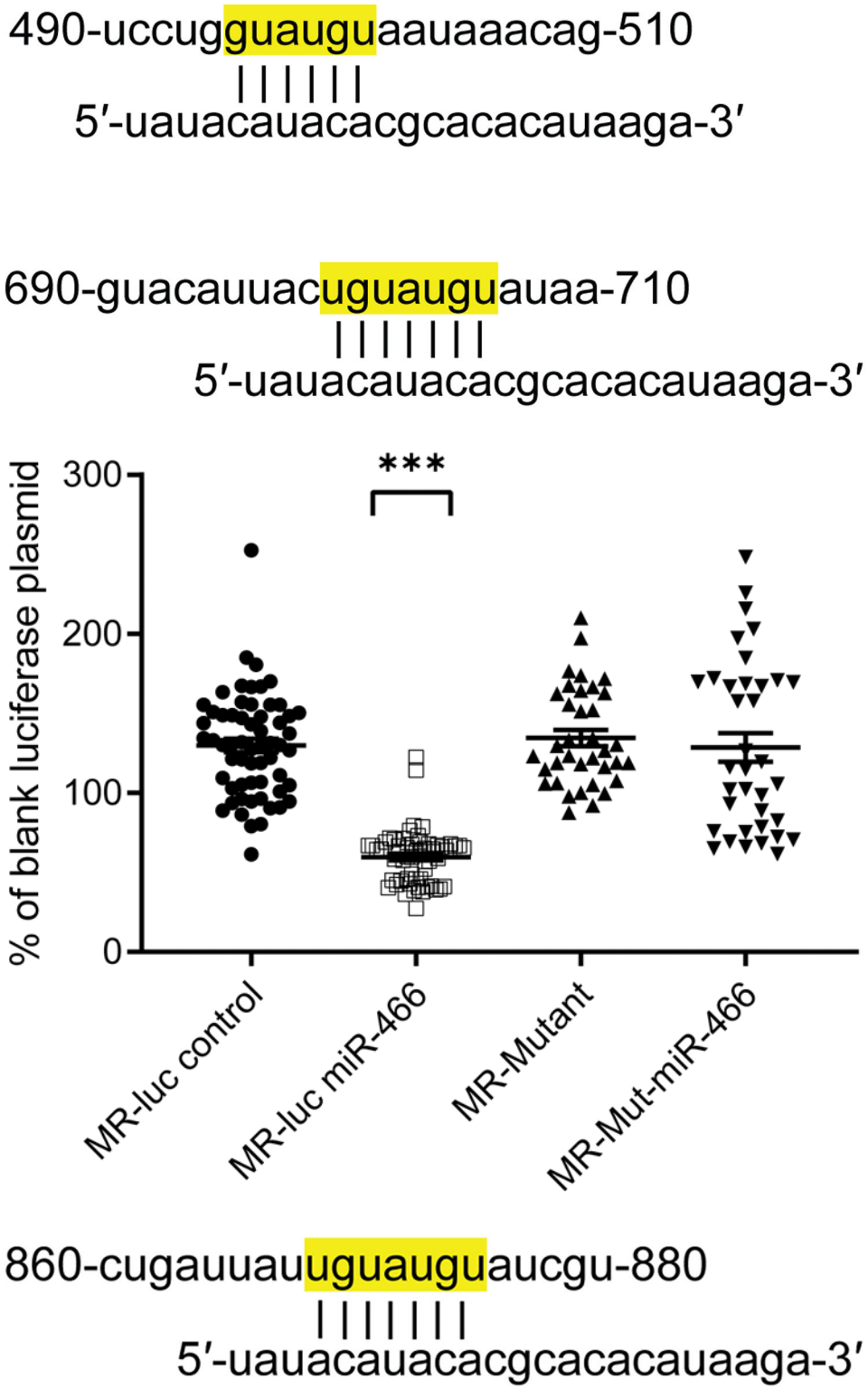

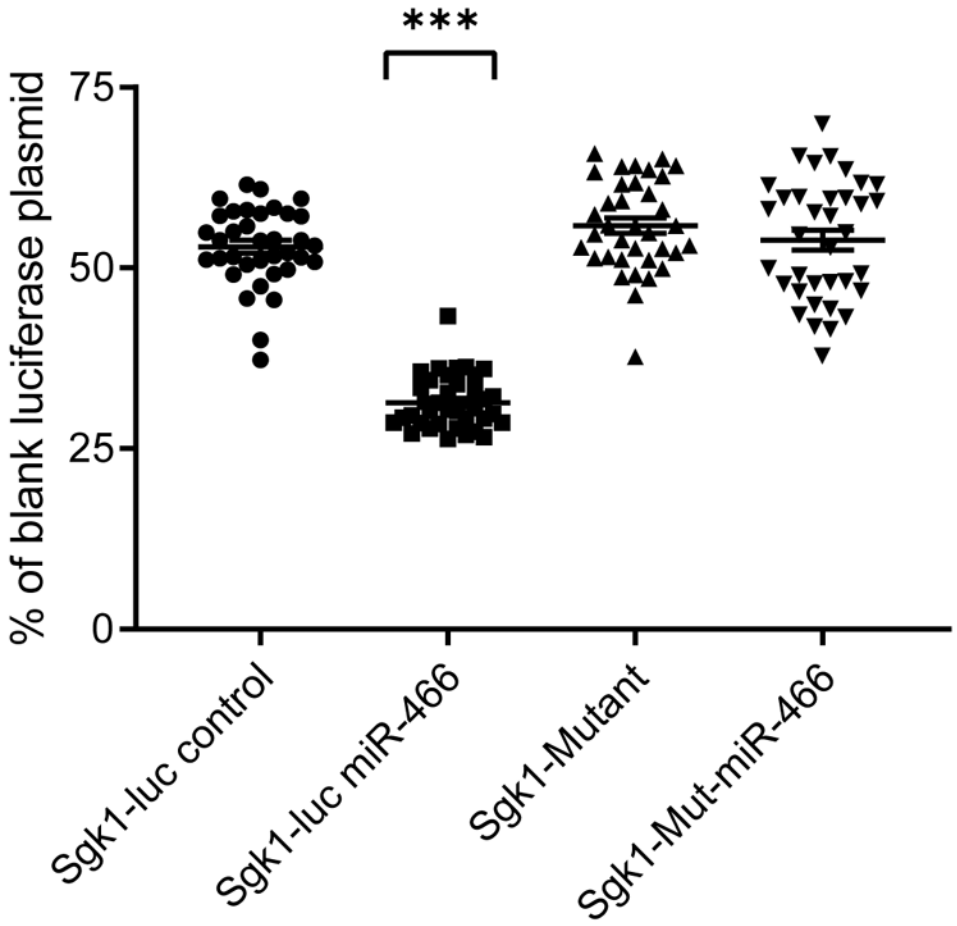

Figure 2:

A) Predicted miR-466 binding sites on the MR-3'UTR (mouse NR3C2) that were eliminated in the MR-mutant construct (MR-Mut). B) Dual luciferase assay for MR luciferase constructs transfected into HEK cells with control or miR-466 mimic (50nM). Luciferase signal was normalized to the second (non-targeted) luciferase reading and expressed as a % of the blank (pmiR-Glo) luciferase signal (N=4 replicates,*** $p<0.001$, one-way ANOVA). C) Predicted miR-466 binding site on the SGK1-3'UTR (mouse SGK1) that was eliminated in the Sgk1-mutant construct (Sgk1-Mutant). D) Dual luciferase assay for SGK1 luciferase constructs transfected into HEK cells with control or miR-466 mimic (50nM). Luciferase signal was normalized to the second (non-targeted) luciferase reading and expressed as a % of the blank (pmiR-Glo) luciferase signal (N=3 replicates,*** $p<0.001$, one-way ANOVA).

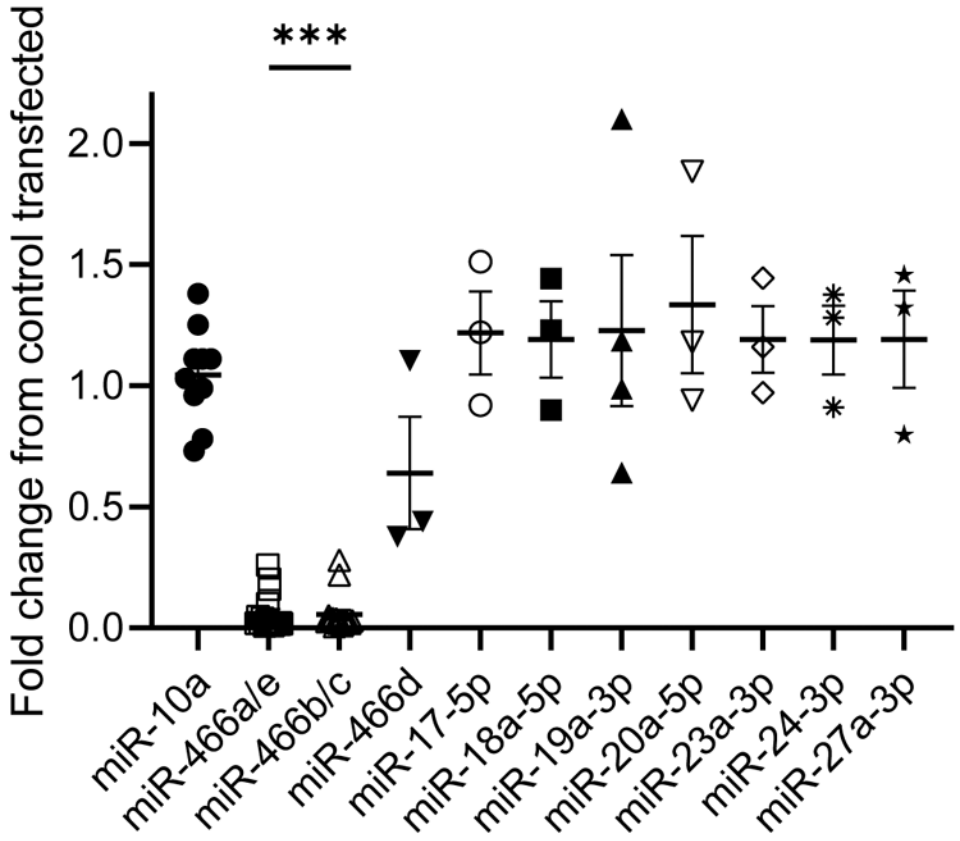

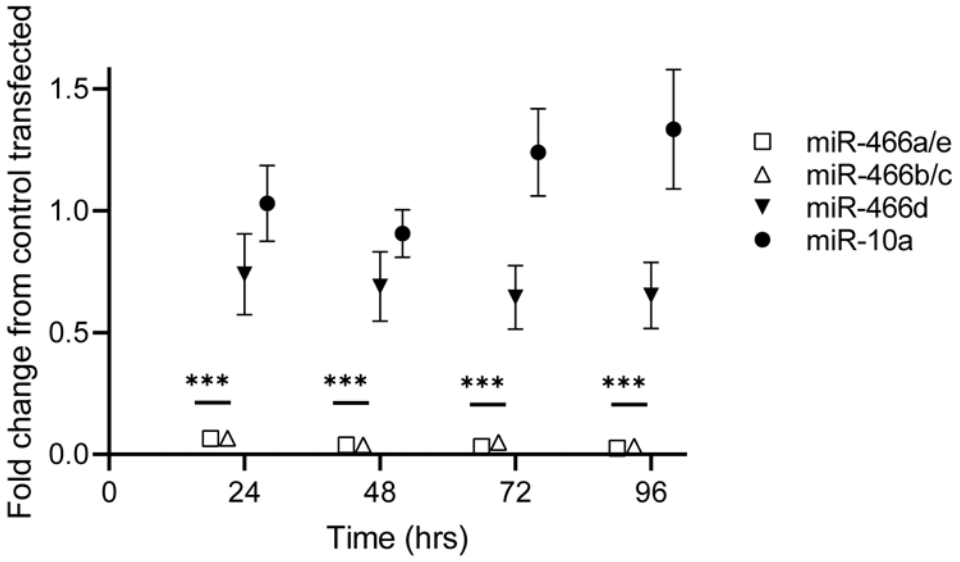

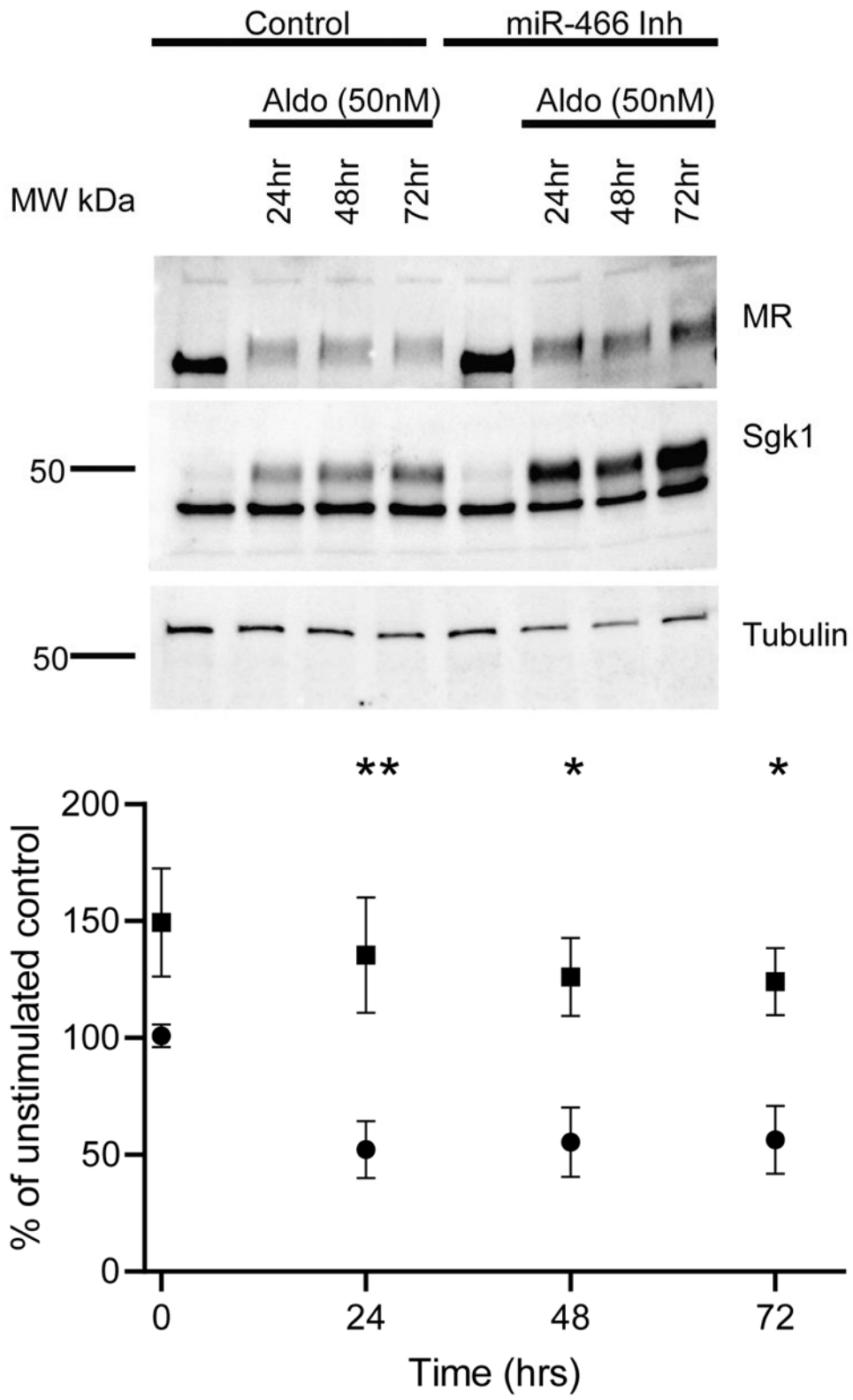

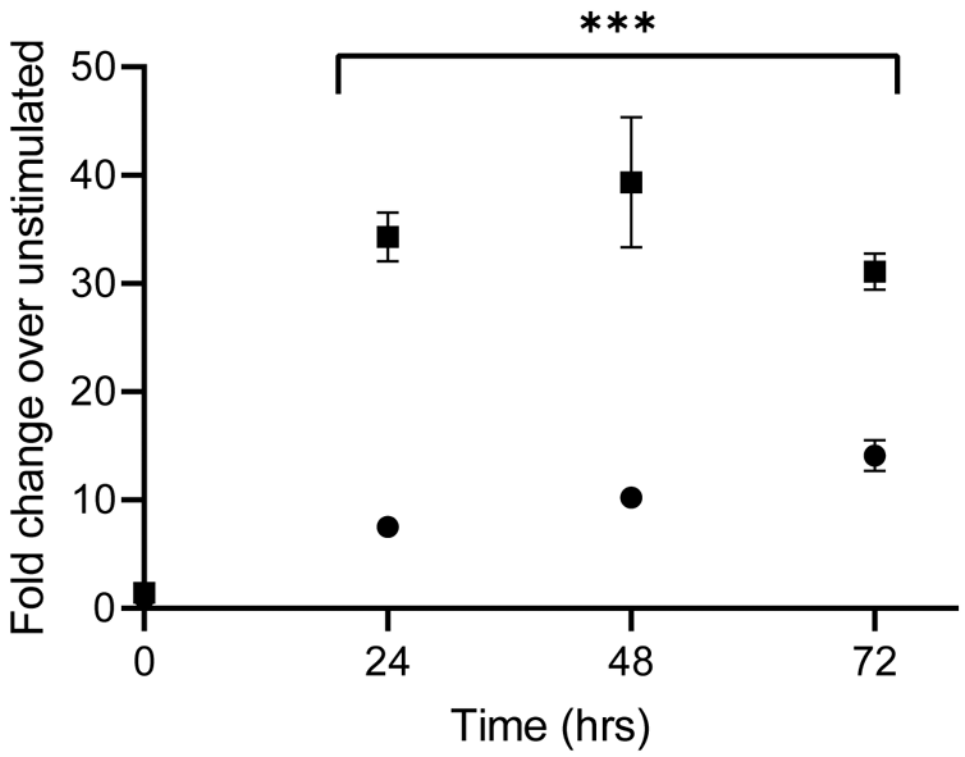

Figure 3:

A) qRT-PCR expression of miR-466 family members and unrelated miRs in mCCD-cl1 cells transfected with a miR466 antagomir (50nM) compared to control transfected cells. No significant change in the expression of non-targeted miRs was noted whereas miR-466a/e and b/c family members showed a significant decrease in relative expression 24 hrs post transfection (***=p<0.001, one-way ANOVA). B) A timecourse of miR-466 expression in mCCD cells following transfection of miR-466 antagomir (at time = 0 hrs). MiR-466 a/e & b/c expression remained repressed to 96 hrs, with no significant change to control miR-10a or non-targeted miR-466d (***=p<0.001 compared to control expression, one-way ANOVA). C) Western blot of MR and SGK1 from whole cell lysates from mCCD cells transfected with miR-466 antagomir or control RNA, stimulated with 50nM aldosterone for 24-72 hrs. The shift in MR apparent molecular weight (~100kDa) is due to posttranslational modifications in MR with aldosterone stimulation. D) Densiometric quantification of MR, bands were normalized to tubulin and expressed as a *percentage* of control unstimulated levels (Closed circles = control, closed triangles = miR-466 inhibited, N=5 biological replicates.**=p<0.01, *=p<0.05 relative to control transfected, one-way ANOVA). E) Densiometric quantification of SGK1 bands were normalized to tubulin and expressed as a *fold* change from control, unstimulated protein levels. No significant difference in unstimulated SGK1 protein levels between control and miR-466 inhibited mCCD was observed (points overlap at t=0 hrs, error bars too small to display). SGK1 protein levels are significantly greater in miR-466 inhibited cells than control transfected at each timepoint (Closed circles = control, closed triangles = miR-466 inhibited, p<0.001, one-way ANOVA, N=5).

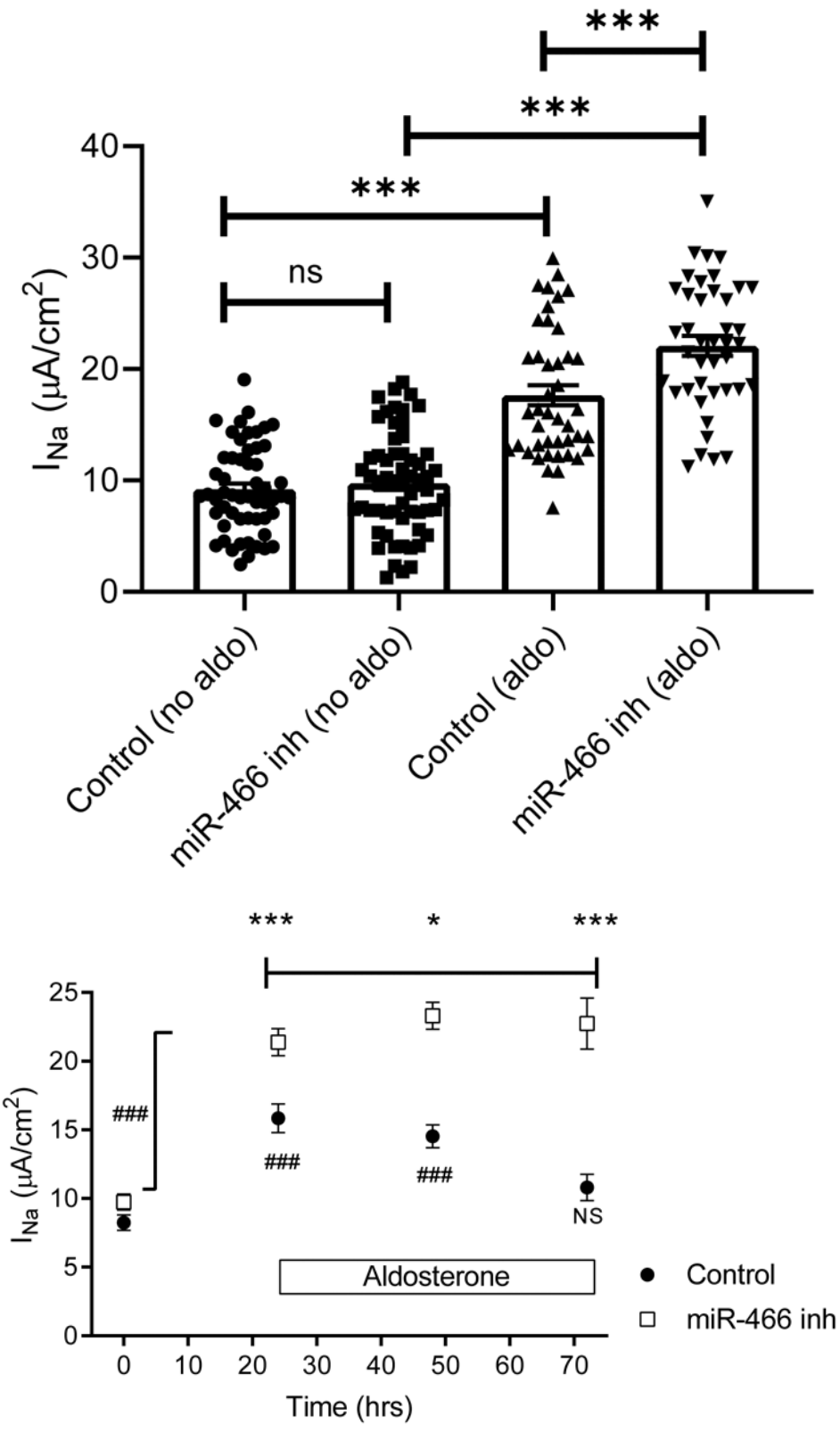

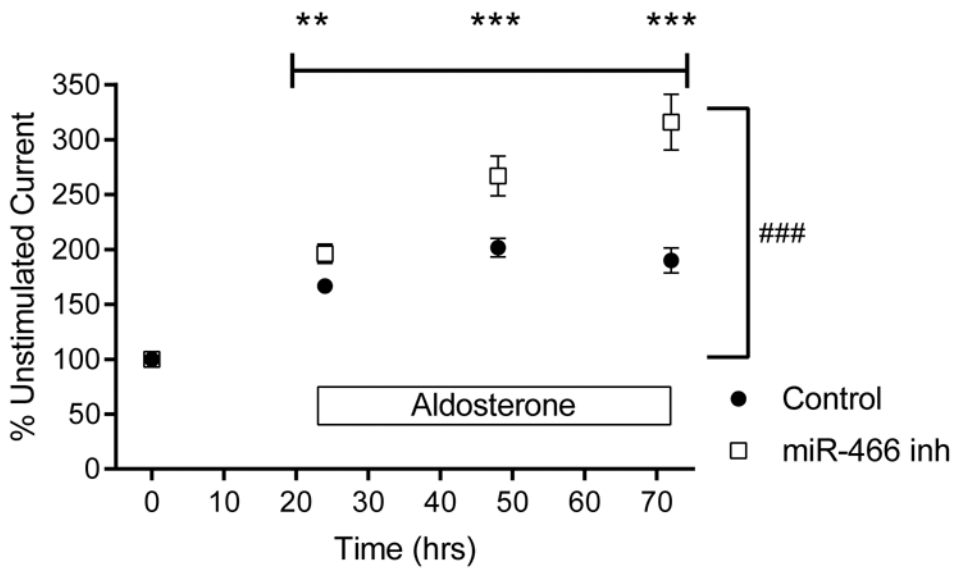

Figure 4:

A) Summarized amiloride-sensitive short-circuit current (I_{Na}) from mCCD cells mounted in Ussing chambers. Cells were transfected with the miR-466 antagomir (miR-466 inh) or control RNA and stimulated with 50nM aldosterone for 24 hrs, amiloride (10μM) was added to determine the I_{Na}. *** indicates significant difference ($p<0.001$), ns = no significant difference (N=8, n>30, one-way ANOVA). B) Summarized I_{Na} from control and miR-466 inhibited mCCD cells stimulated with aldosterone (50nM) for 24-72 hrs. Maximum I_{Na} in control cells declined by 72 hrs but remained elevated in miR-466 inhibited cells. *** ($p<0.001$) or * ($p<0.05$) indicates significant difference compared to control transfected at the same time point, ### indicates significant difference ($p<0.001$) compared to unstimulated (N=8, n=15-62, one-way ANOVA). C) Currents expressed as a percentage of unstimulated cells for each day of recording for each group. *** ($p<0.001$) or ** ($p<0.01$) indicates significant difference compared to control transfected at the same time point, ### indicates significant difference ($p<0.001$) compared to unstimulated (N=8, n=15-62, one-way ANOVA).

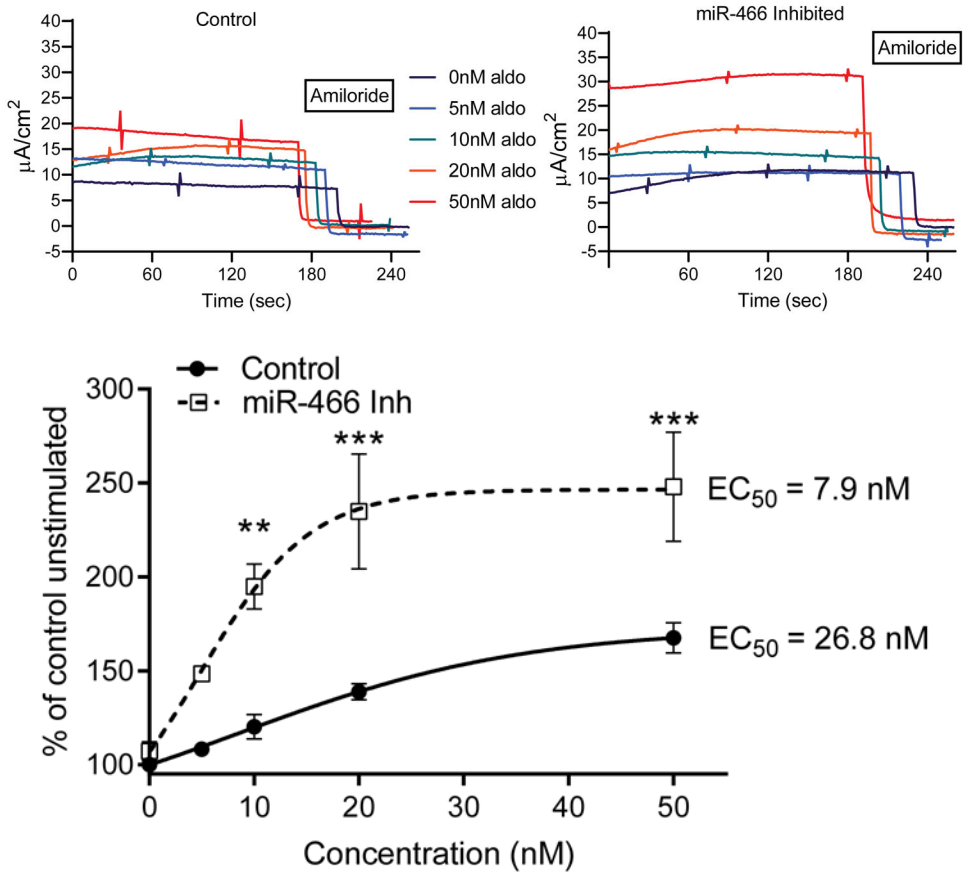

Figure 5:

A) Representative short-circuit current traces from control (left) and miR-466 inhibited (right) mCCD cells treated with increasing doses of aldosterone (indicated by colored traces) for 24 hrs. Amiloride (10μM) was added at the end of each recording to determine the I_{Na}. B) Dose response to increasing aldosterone concentration expressed as a % increase in I_{Na} of the unstimulated currents. The calculated EC_{50} for aldosterone stimulation is 26.8nM for control and 7.9nM for miR-466 inhibited cells. ** = $p<0.01$ or *** = $p<0.001$ indicates significant difference from control transfected mCCD cells (N=5, n=10-27 for each point, one-way ANOVA and non-linear fit).

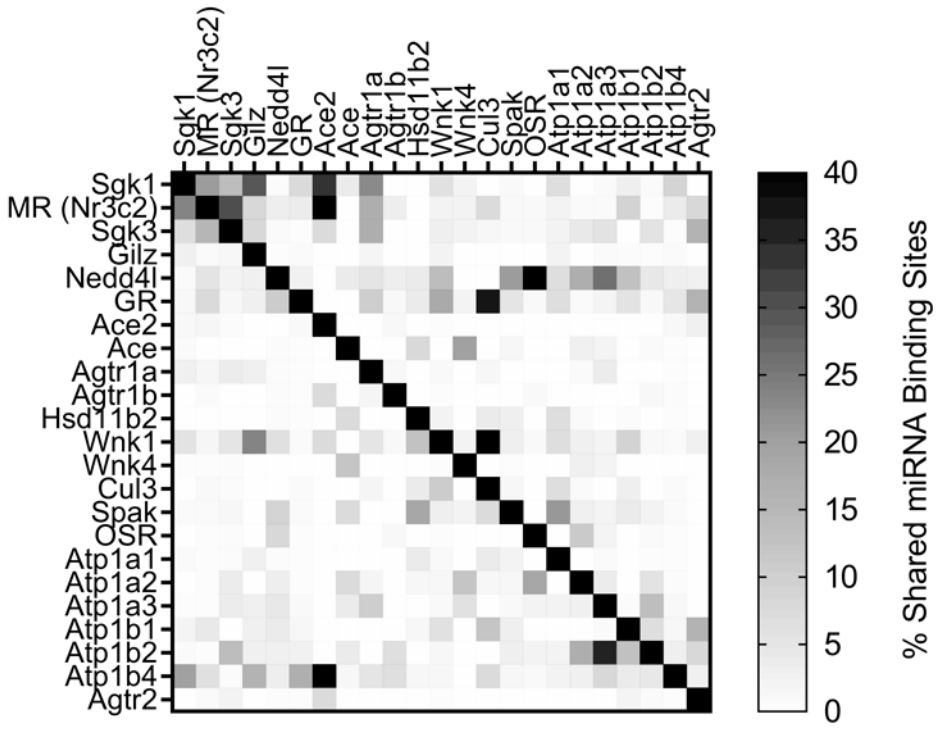

Figure 6:

Heatmap of % of miRs predicted to bind to the mRNAs listed (from miRDB predictions). The higher the number of miRs shared between the targets, the darker the square. As an example, SGK1 (top left) is predicted to share 33% of the miRs that bind to Ace2, but 0% (no miRs) of the miRs predicted to bind to SGK1 are predicted to target Cul3 or OSR.

Table 1.

Table listing sequences of primers, oligonucleotides and summary of the qPCR protocol used in the study

qPCR primers		
Gene	**Forward primer sequence**	**Reverse primer sequence mouse**
Actin	5’-GCAGCTCCTTCGTTGCCGGT-3’	5’-GGGGCCACACGCAGCTCATT-3’
GAPDH	5’-CATCACCATCTTCCAGGAGCG-3’	5’-GAGGGGCCATCCACAGTCTTC-3’
SGK1	5’-CTGCTCGAAGCACCCTTACC-3’	5’-TCCTGAGGATGGGACATTTTCA-3’
αENaC	5’-GCTCAACCTTGACCTAGACCT-3’	5’-GGTGGAACTCGATCAGTGCC-3’
Nedd4–2	5’-TTGGTGATGTCGACGTGAACGACT-3’	5’-TGGAGGTGCCTGTGACAAACTGTA-3’
NR3C2	5’-CAACTATCTGTGTGCTGGAAGA-3’	5’-CCTTGGTAGGAGCAATGTATGT-3’
NR3C1	5’-CCTTCGGGAGCTTTAGGTTT-3’	5’-GCAGGGTATTTAGGAGGGTATTT-3’

microRNA	***Primer Sequence***
mmu-let-7a-1-3p	CTATACAATCTACTGTCTTTCC
mmu-let-7b-3p	CTATACAACCTACTGCCTTCCC
mmu-let-7c-2-3p	CTATACAATCTACTGTCTTTCC
mmu-let-7f-1-3p	CTATACAATCTATTGCCTTCCC
mmu-miR 10a	TACCCTGTAGATCCGAATTTGT
mmu-miR-101b-3p	GTACAGTACTGTGATAGCT
mmu-miR-127-5p	CTGAAGCTCAGAGGGCTCTGAT
mmu-miR-135a-5p	TATGGCTTTTTATTCCTATGTGA
mmu-miR-186-5p	CAAAGAATTCTCCTTTTGGGCT
mmu-miR-19a-3p	TGTGCAAATCTATGCAAAACTGA
mmu-miR-204-5p	TTCCCTTTGTCATCCTATGCCT
mmu-miR-211-5p	TTCCCTTTGTCATCCTTTGCCT
mmu-miR-216b-3p	ACACTTACCTGTAGAGATTCTT
mmu-miR-28a-3p	CACTAGATTGTGAGCTGCTGGA
mmu-miR-365-3p	TAATGCCCCTAAAAATCCTTAT
mmu-miR-466a-3p	TATACATACACGCACACATAAGA
mmu-miR-466b-3p	ATACATACACGCACACATAAGA
mmu-miR-466c-3p	ATACATACACGCACACATAAGA
mmu-miR-466e-3p	TATACATACACGCACACATAAGA
mmu-miR-466p-3p	ATACATACACGCACACATAAGA
mmu-miR-467c-3p	ATATACATACACACACCTATAC
mmu-miR-467d-3p	ATATACATACACACACCTACAC
mmu-miR-467e-3p	ATATACATACACACACCTATAT
mmu-miR-669d-2-3p	ATATACATACACACCCATATAC
mmu-miR-669d-3p	TATACATACACACCCATATAC
mmu-miR-669l-3p	ATATACATACACACCCATATAT

microRNA	*Primer Sequence*
mmu-miR-669m-3p	ATATACATCCACACAAACATAT
mmu-miR-669n	ATTTGTGTGTGGATGTGTGT
mmu-miR-6715-3p	CCAAACCAGGCGTGCCTGTGG

MicroRNA mimic and Inhibitor		
miRNA	**Sequence**	
miR 466b-3p	5’-AUACAUACACGCACACAUAAGA-3’	
miR 466b-3p Inhibitor	5’-CUUAUGUGUGCGUGUAUGUA-3’	
miR negative control	5’-ACCAUAUUGCGCGUAUAGUCGC-3’	
qPCR protocol	**50°C- 2min**	
	95°C −2min	
	40 cycles 95°C 15s, 60°C 1min	

Table 2.

Table listing tested miRNAs predicted to bind to the mouse Nr3c2 3'-UTR, ranked from highest to lowest (by miRDB.org). The equivalent ranking from Diana Tools is presented (where available, ND=not determined). The change in miRNA expression from mCCD cells cultured on filter supports and stimulated with aldosterone (50nM for 24 hrs) compared to unstimulated levels (n=3) is expressed as a relative fold change (SEM=standard error of the mean)

miRBD Target Score	miTG score (Diana Tools)	miRNA Name	Fold Change (24 hrs Aldo)	SEM
99	94	mmu-miR-669n	0.86	0.02
95	82	mmu-miR-466b/c-3p	1.89	0.60
95	82	mmu-miR-466p-3p	1.13	0.26
95	93	mmu-miR-124-3p	1.06	0.08
93	85	mmu-miR-216b-3p	1.02	0.01
92	83	mmu-miR-669d-2-3p	0.94	0.15
92	85	mmu-miR-467c-3p	0.81	0.21
92	85	mmu-miR-467d-3p	0.80	0.14
92	95	mmu-miR-204-5p	0.78	0.19
92	95	mmu-miR-211-5p	0.83	0.16
92	85	mmu-miR-467e-3p	0.54	0.00
92	71	mmu-miR-669m-3p	0.92	0.05
92	83	mmu-miR-669l-3p	0.92	0.27
92	99	mmu-miR-365-3p	0.96	0.12
89	ND	mmu-miR-127-5p	0.80	0.32
85	98	mmu-miR-19a-3p	1.39	0.15
85	99	mmu-miR-135a-5p	0.84	0.05
83	98	mmu-miR-466a/e-3p	1.95	0.58
83	97	mmu-miR-669d-3p	0.94	0.15
78	83	mmu-miR-6715-3p	1.12	0.17
69	82	mmu-miR-186-5p	1.19	0.11
64	ND	mmu-let-7a-1-3p	0.88	0.14
64	ND	mmu-let-7b-3p	0.78	0.09
64	ND	mmu-let-7c-2-3p	0.85	0.09
64	ND	mmu-let-7f-1-3p	0.76	0.12
61	80	mmu-miR-28a-3p	1.15	0.15
60	ND	mmu-miR-101b-3p	0.89	0.16